

FULL WAVEFORM ANALYSIS: ICESAT LASER DATA FOR LAND COVER CLASSIFICATION

Hieu Duong, Norbert Pfeifer and Roderik Lindenbergh

Delft University of Technology, Delft Institute of Earth Observation and Space systems, The Netherlands
(h.vanduong, r.c.lindenbergh)@lr.tudelft.nl
alpS - Centre of Natural Hazard Management, Innsbruck, and Institute of Geography, University of Innsbruck, Austria
norbert.pfeifer@uibk.ac.at

Commission VII

KEY WORDS: Full waveform, laser scanning, ICESat, land cover classification.

ABSTRACT:

Analysis of the full waveform return pulse of laser altimeter systems is expected to increase the possibilities and accuracy in well-known applications of laser altimetry like DTM generation, forestry and earth surface analysis. NASA's ICESat Geoscience Laser Altimeter System (GLAS) was launched in 2003 and acquires full waveform data along profiles covering the entire earth. In this study, the possibility of using ICESat data for land-cover classification is investigated over the Netherlands using data obtained from September to November 2003. The method, that automatically analyzes raw waveforms, divides the footprints of the laser pulses in four categories: high vegetation (high trees or forest), urban, water, and bare land/low vegetation. First, Gaussian components are fitted to and then several parameters derived from the Gaussian decomposition are used for discriminating the land-cover layers. Finally, the accuracy of the land-cover classes is validated by computing a confusion matrix based on the CORINE land cover database 2000 (CLC2000) covering the same study area. Using our method we get 73% accuracy of classification.

1. INTRODUCTION

Creating land cover databases is one of the most important targets in remote sensing. Land cover assessment and monitoring of its dynamics are essential requirements for sustainable management of natural resources and for environmental protection. They provide the foundation for environmental, food and humanitarian programmes of international and national. Accurate, detailed, and reliable land cover information remains in demand (GLCN-LCTC, 2006).

Remotely sensed images are the main source of data used for land cover classification. The images are acquired from different platforms as satellite, airplane or ground, from different systems both passive and active, and from various sensors with different resolutions. In this article, we consider the possibilities that the ICESat mission has as a new source for land cover data. For this purpose we develop a method of classification. The classified results of ICESat data are validated by comparison to the CORINE land cover database.

ICESat was launched in January 2003 with the principal objectives to measure: polar ice-sheet elevation change; atmospheric profiles of cloud and aerosol properties; land topography profiles referenced to a global datum; and height of vegetation canopies. These objectives are accomplished using the Geoscience Laser Altimeter System (GLAS) combined with precise orbit determination. GLAS uses a laser altimeter to measure the range distance between the satellite and the earth surface. GLAS systematically samples the energy profile returned from the surface as a full waveform (Harding and Carabajal, 2005). ICESat data can therefore only be used for classifying profiles, as compared to regions mapped by area-sensors. The full waveform data gives new possibilities to extract more information about land cover of the earth surface.

In this study, the full waveform analysis is investigated in the context of land cover classification. The paper suggests a new and potential way to extract land cover classes from the full waveform data. Firstly, the waveform is assumed to be a sum of Gaussian components. The waveform is then decomposed into different Gaussian components. Next, the waveform parameters derived

from the decomposition are applied in the classification step to identify land cover type. Moreover, the quality of the fitting step is also analyzed. The footprints are classified independently of each other.

In the next section, we will introduce our study area, the ICESat/GLAS dataset and a reference land cover map. Then we will introduce new methodology for analyzing full waveform data with the purpose of land cover classification. In the results section we will give the total accuracy of the classification based on computing a confusion matrix between the ICESat data and the reference data. Finally, conclusions will be stated at the end.

2. STUDY AREA AND DATASET

2.1 Study area

The area of study is mostly the Netherlands, bounded approximately by $3^{\circ}E$ to $7^{\circ}E$ longitude and $50^{\circ}N$ to $54^{\circ}N$ latitude which contains a large variety of land cover. There are 15 products of ICESat data, however, only the products GLA14 and GLA01 in release 24 are used for this research. The GLA14 contains precise geolocation of footprint centers with height information. The GLA01 contains the full captured waveform. Release 24 means that these products are processed using currently the most recent version of the NASA processing procedure. A GLA01 waveform is linked to a GLA14 location by index and shot number. The index and shot number are computed by relating the shooting time of an individual pulse to the starting time of the ICESat operation and the shooting frequency. The waveform locations are displayed together with a CORINE land cover map in Figure 1.

2.2 ICESAT/GLAS full waveform data

GLAS was designed for a 183-day ground track repeat cycle with 7.5 km spacing between the repeated tracks at 60 degree latitude. However, due to the problems of the laser system, GLAS changed to operate in a 91-day repeat orbit to complete a global coverage (Ranson, Sun, Kovacs, and Kharuk, 2004). Both data from ascending and descending orbits are used in this study. A visualization of the footprint sizes is shown in Figure 2.

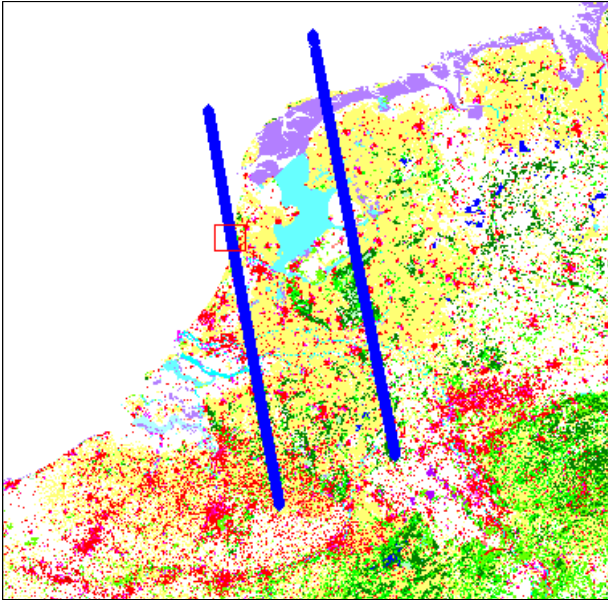


Figure 1. Study area: ICESat ground tracks (blue) and CLC2000 land cover map (100m resolution)

The full waveform dataset was acquired in the period from 2003-09-25 to 2003-11-18. There are 3277 waveforms in the study area. The footprints of these waveforms are elliptical, its power distribution has a central maximal, while energy decreases to the boundary. The size of the ellipse is 95 x 52m on average (Harding and Carabajal, 2005). The footprint separation is 175m along track. The horizontal geolocation accuracy of the ICESat footprints is 3.7m. The waveform is digitized in 544 nanoseconds over land area and 200 nanoseconds over sea or ocean. That means that the waveform can acquire a height of up to 81.6m over land and 30m over sea with the vertical resolution of 15cm.

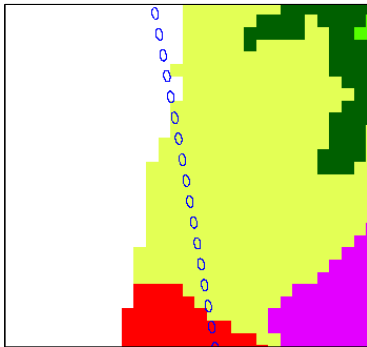


Figure 2. A close up of the red rectangle in Figure 1 with elliptical footprints of 95 x 52 m. The track passes from the North Sea (in white) onto land (in color).

2.3 CLC2000 land cover data

The CORINE Land Cover 2000 database (CLC2000) is used as reference data for an accuracy assessment of the classification results. The land cover database is dated to the year 2000 but actually was obtained during a 3 years period from 1999 to 2001 with a horizontal geolocation accuracy of worse than 25m based on IMAGE2000 and a resolution of 100m. The CLC2000 classification is hierarchical and distinguishes 44 classes at the third level, 15 classes at the second level and 5 classes at the first level. De-

tailed information of land cover levels can be found at the metadata section of CLC2000 in the European Environment Agency website (CLC2000, 2006). The total thematic accuracy of the CLC2000 database is almost 95% and meets the European target of 85%. The database is geo-referenced in the European reference system (Hazeu, 2003).

3. WAVEFORM PARAMETERIZATION AND QUALITY ASSESSMENT

3.1 Pre-processing and initialization

Due to different reference systems of both ICESat and CLC2000, a conversion of the reference system is taken into account. The ICESat data is therefore converted to a common reference system ETRS89 by ArcGIS 9.0 software.

The binary data of GLA01 and GLA14 is converted into ASCII format by an IDL program developed by the National Snow and Ice Data Center (NSIDC, 2006). The waveform data that is originally in counts (from 0 to 255) is converted into voltage units for further analysis.

The voltage waveform is then normalized by dividing by the total received energy. This implies that the area under any normalized waveform equals one. Next, the normalized waveform is further smoothed. Finally, the smoothed waveform is used for estimation of the Gaussian parameters in the fitting step.

3.2 Gaussian fitting

In the fitting step, so-called Gaussian components are fitted to the normalized and smoothed waveform $w(t)$. Every Gaussian component $W_m(t)$ corresponds to one Gaussian bell curve. So, we assume that the smoothed waveform $w(t)$ is a sum of Gaussian components $W_m(t)$. That is, we write

$$w(t) = \sum_{m=1}^{N_p} W_m(t), \quad \text{with} \quad W_m(t) = A_m e^{-\frac{(t-t_m)^2}{2\sigma_m^2}}, \quad (1)$$

where $w(t)$ is the amplitude of the waveform at time t , $W_m(t)$ is the contribution of the m -th Gaussian component, N_p is the number of Gaussians found in the waveform, A_m is the amplitude of the m -th Gaussian, t_m its position and σ_m its standard deviation. In Figure 3, the normalized waveform is given in red, the smoothed waveform is in gray and the fitted waveform is in black. The found Gaussian components are displayed in green. A detailed description of this fitting step and the preprocessing are found in (Duong, Pfeifer, and Lindenberg, 2006).

3.3 Quality of fitting

A waveform normally has 544 bins over land, but by visualization of the dataset we know that the actual waveform often starts after the 150th bin or after 150 nanoseconds. Therefore, the first 150 bins of the waveform can be used to determine the noise component of the waveform signal. For validating the quality of fitting, two noise levels are taken into account: local noise and global noise. For the local noise the noise in the first 150 bins of every raw waveform is used to calculate a standard deviation, the so-called σ_{N_i} (the index i stands for the i^{th} waveform.). The global noise is the mean local noise of the entire waveform dataset, the so-called $\bar{\sigma}_N$. These parameters of σ_{N_i} and σ_{WF_i} are depicted in Figure 4.

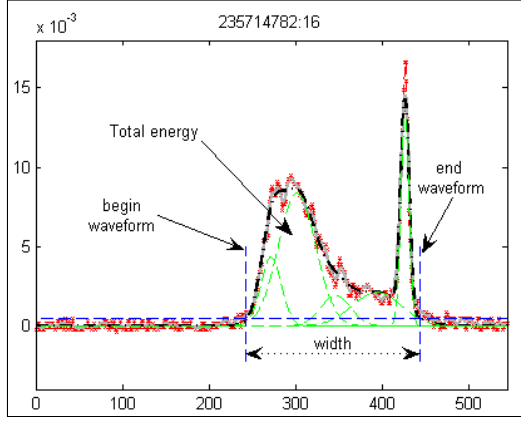


Figure 3. A typical waveform with parameters as begin point, width, total energy, and number of modes.

Moreover, the remaining bins of the waveform are used to define two other notions that allow validation of the quality of fitting: σ_{WF_i} and $\bar{\sigma}_{WF}$. The σ_{WF_i} is the local standard deviation of the waveform and is defined as the mean of the bin-wise differences between the actual waveform and the sum of the fitted Gaussian components. The actual waveform is that part of the waveform between the begin point and end point in Figure 3. These points are obtained using a suited threshold value. The $\bar{\sigma}_{WF}$ is the mean waveform standard deviation of the entire dataset. Figure 3 and Figure 4 show the location of the actual waveform as bounded by the dashed blue vertical lines. The locations of these lines are identified by truncating the fitted waveform (dashed black curve) by a threshold value based on the local noise intensity (horizontal dashed blue line) in Figure 3.

To access the quality of the fitting of the waveform, the four described parameters of above are used: the noise standard deviation σ_{N_i} , the waveform standard deviation σ_{WF_i} , the mean noise standard deviation $\bar{\sigma}_N = \frac{1}{N} \sum_{i=1}^N \sigma_{N_i}$, and the mean waveform standard deviation $\bar{\sigma}_{WF} = \frac{1}{N} \sum_{i=1}^N \sigma_{WF_i}$, where N is the number of waveforms in the entire dataset.

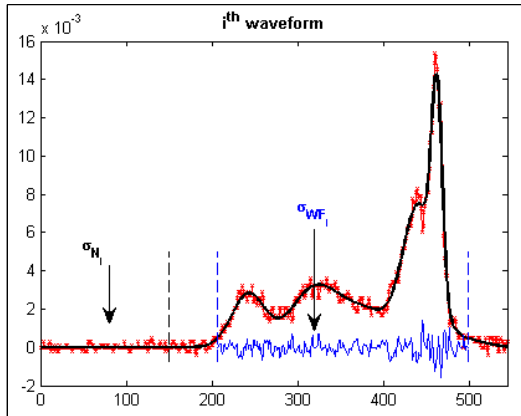


Figure 4. A waveform with noise standard deviation σ_{N_i} (from 1 to 150 nanoseconds) and waveform standard deviation σ_{WF_i} (in blue). The noise range is from 1 to 150 nanosecond (at vertical dashed black line). The actual waveform is located between the two vertical blue lines.

The quality of the fitting is validated and displayed in Figure 5. The x-axis is the ratio of σ_{WF_i} and σ_{N_i} . The y-axis is the percentage of waveforms fitted. The continuous and dashed black

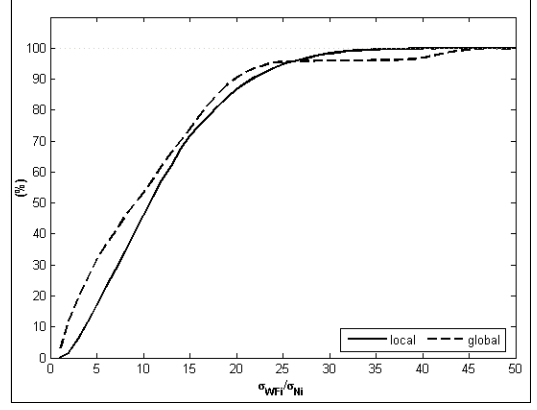


Figure 5. Quality of fitting in terms of the noise standard deviation: the solid curve (local) and dashed curve (global).

curves represent the local and global level. Figure 5 shows that the results for the quality of fit using either local or global noise are similar. 95 per cent of the waveforms is fitted well within 25 times σ_{N_i} or within 23 times $\bar{\sigma}_N$. Therefore, selection of the local and global noise will give the same result in validating the quality of fit. Moreover, in terms of mean standard deviations of waveform and noise, we get $\sigma_{WF} = 10.8\bar{\sigma}_N$.

3.4 Waveform parameters for classification

The fitting step results in a number of Gaussian components with Gaussian parameters. However, for the classification purpose, other parameters are also helpful: *width* and *total energy*.

Due to the existing noise in the waveform, the actual width of the waveform or the actual waveform needs to be identified by finding the locations of the actual begin and end of the waveform. The threshold value for each waveform is defined by taking the maximum value of the (noise) intensity in the first 150 bins. This threshold value is applied to truncate the waveform by specifying the locations of the actual begin and end of the waveform. Therefore, the begin of the waveform is the intersection of the horizontal threshold value line and the first rising edge of the waveform (most left). The end point of the waveform is the last intersection point (most right). The width of the waveform is the distance between the begin and the end location of the waveform. A visualization of the width and the actual waveform is shown in Figure 3 and Figure 4.

Four waveform parameters are used in the classification step: **NModes**: Total number of Gaussians as found by the fitting algorithm. **TEnergy**: Total energy received back by the GLAS instrument. This is calculated by taking the area under the actual waveform. The result is converted in energy units (attojoules = 10^{-18} joules). **BeginWF**: Location where a waveform firstly passes the threshold. **Width**: Width is the distance between the begin and the end of the actual waveform.

Again, in Figure 3, the red line represents the normalized waveform. The dashed black line represents the fitted waveform with in this case 5 Gaussian modes. The different Gaussian components are displayed by dashed green lines.

4. WAVEFORM CLASSIFICATION

The four waveform parameters described in the above section are used in the classification step. Waveforms are classified into 4

different classes: *high vegetation*, *urban*, *bare land/low vegetation* and *water*. The flowchart for this classification is shown in Figure 6.

Water normally absorbs the energy of the laser, therefore the energy of the recorded waveform over water is mostly lower than over bare land, urban or high vegetation. Therefore the total energy is used to extract water waveforms.

Bare land has a flat open surface, so it mostly gives uni-mode waveforms. Moreover, bare land can also cause the recorded waveform to have a wider width due to roughness or slope of the surface. Low vegetation can result in waveforms having multi-modes. However the extra modes have low amplitude and will be few. In this particular step, the bare land waveforms are classified by having only one mode. Moreover, by regarding the effect of low vegetation, bare land waveforms are selected in the next step by having a narrower waveform width.

Urban and high vegetation are known as complex areas with different height levels. Therefore, the area usually results in multi-mode and wide-width waveforms. This is caused both by artificial objects as well as by high trees. However, waveforms over high vegetation often have a wider first mode width due to the scattering from the tree crowns. The urban waveform has a narrower width for all modes due to the reflectance from the sharp shape of artificial objects like buildings, etc. In other words, the wider first mode results in an earlier rising of the first edge of the actual waveform. In this case, the location of the waveform start is used to separate urban from high vegetation waveforms. Four representative waveforms for four different land cover classes are shown in Figure 7.

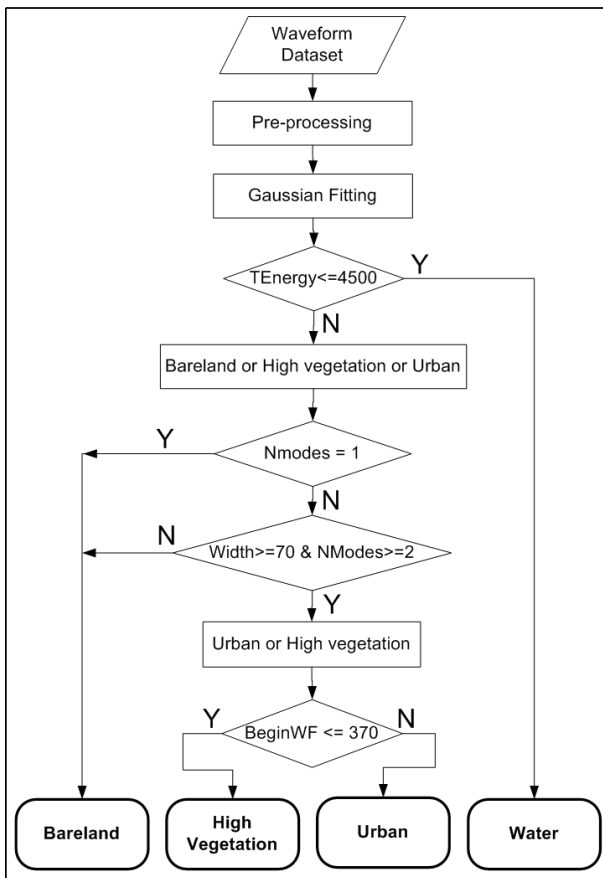


Figure 6. Flowchart of a classification step.

5. CLASSIFICATION VALIDATION AND RESULTS

From the point of view of image processing, a waveform data with ellipsoidal footprint size of 95x52 m can be approximated by a polygon that contains a number of pixels within its boundary. The polygon of the classified waveform represents the polygon of pixels in the classified image. The CLC2000 reference data with 100m resolution, is used for validation and represents a known land cover type. Moreover, the CLC2000 is splitted into 25m pixels that inherit the pixel values of the full 100m pixel. In this way, we obtain a larger number of pixels within the footprint polygon, which helps in the accuracy assessment. For example, the footprint polygon overlaps two reference pixels of 100m resolution. The first reference pixel has a large common area and the second has a small common area with the footprint polygon. When using reference data of 100m resolution, only two reference pixels are selected. However, if we use 25m resolution reference data, we can have more pixels of 25m in the first reference pixel and less in the second one, which improves the precision of the results.

5.1 Confusion matrices

One of the common means of expressing classification accuracy is the preparation of a classification *confusion matrix* (also called error matrix or contingency table) (Lillesand, Kiefer, and Chipman, 2004). A confusion matrix compares, on a category-by-category basis, the relationship between known reference data (ground truth) which is here the CLC2000 data and the corresponding results to be validated, here the classification of the ICESat data. The matrices are squared, with the numbers of rows and columns equal to the number of categories or classes whose classification accuracy is being assessed. The matrix shows how well a classification is categorized, but also how bad the classification errors of omission and commission are.

A commission error means that a pixel is falsely classified within a certain class. In this research, the commission error for water consist of 1394 pixels that are falsely classified as not water. 644 are classified as bare land, 706 as high vegetation and 44 as urban. An omission error occurs when a pixel is falsely omitted from a class by the classifier method. Thus, the classification based on full waveform laser altimetry analysis fails to recognize and correctly identify 589 from 3162 as not water.

Several other descriptive measures can be obtained from the confusion matrix. The *overall accuracy* is the probability that a pixel randomly taken from the classified data has the same class as the corresponding pixel in the reference data and vice versa. The overall accuracy is computed by dividing the total number of correctly classified pixels (the sum of the elements along the major diagonal) by the total number of reference pixels.

The *producer's accuracy* is the probability that a pixel taken randomly from reference data class *i* has the same class as the corresponding pixel in the classified data. It indicates how well the reference data of the class are classified. The producer's accuracy results from dividing the number of correctly classified pixels in each class by the number of reference pixels used for that class (the column total).

Finally, the *user's accuracy* is the probability that a pixel taken randomly from the classified data class *i* has the same class as the corresponding pixel in the reference data. It indicates the probability that a pixel classified to a class actually represents that class in the reference data. The user's accuracy is computed by dividing the number of correctly classified pixels in each class by the total number of pixels that were classified in that class (the row total).

5.2 Classification validation and results

The CLC2000 data consists of 5 classes at the first level such as *artificial surfaces*, *agricultural areas*, *forest and semi natural areas*, *wetlands*, and *water bodies*. Therefore, the five classes of the CLC2000 data are then reclassified for a suited purpose of the classification validation. Here, the *artificial surfaces* is classified as urban class, the *agricultural areas* and *wetlands* as bare land/low vegetation class, the *forest and semi natural areas* as high vegetation class, and the *water bodies* as water class.

Table 1 shows the confusion matrix between the ICESat and the CLC2000 classification. The columns contain reference data with known land cover type, and the rows are the classified waveform data. The abbreviations of *W*, *B*, *HV* and *U* represent *water*, *bare land/low vegetation*, *high vegetation* and *urban* respectively. Consider for example the water column containing a total number of 3967 water pixels. 2573 are classified correctly as water, 644 are classified incorrectly as bare land, 706 are classified incorrectly as high vegetation, and 44 are classified incorrectly as urban.

Table 2 shows the classification result. The producer's accuracy of the water is 81.37% and the user's accuracy for the water is 64.86%. Moreover, from Table 1, we obtain the overall accuracy of the classification of about 75.22%.

Classification Data	Reference Data				Total
	W	B	HV	U	
W	2573	398	185	6	3162
B	644	1175	457	21	2297
HV	706	1873	7410	216	10205
U	44	81	507	4438	5070
Total	3967	3527	8559	4681	15596

Table 1. Confusion matrix

Class	Prod. Acc. (%)	User Acc. (%)	Prod. Acc. (pixels)	User Acc. (pixels)
W	81.37	64.86	2573/3162	2573/3967
B	51.15	33.31	1175/2297	1175/3527
HV	72.61	86.58	7410/10205	7410/8559
U	87.53	94.81	4438/5070	4438/4681

Table 2. Classification results

The most common parameter for the accuracy assessment is \hat{k} (Lillesand, Kiefer, and Chipman, 2004). The \hat{k} statistic is a measure of difference between the actual agreement between the reference data and an automated classifier on one side and the chance agreement between the reference data and a random classifier on the other side. Conceptually, \hat{k} can be defined as:

$$\hat{k} = \frac{\text{observed accuracy} - \text{chance agreement}}{1 - \text{chance agreement}} \quad (2)$$

where the *observed accuracy* is the proportion of correctly classified entries and the *chance agreement* is the proportion of classes from classification data that could be expected to be classified by chance.

The \hat{k} statistic is computed as

$$\hat{k} = \frac{N \sum_{i=1}^r x_{ii} - \sum_{i=1}^r (x_{i+} \cdot x_{+i})}{N^2 - \sum_{i=1}^r (x_{i+} \cdot x_{+i})} \quad (3)$$

where r is number of rows in the confusion matrix; x_{ii} is an observation in row i and column i (on the major diagonal); x_{i+} is

the total number of observations in row i (shown as marginal total to the right of the matrix); x_{+i} is the total number of observations in column i (shown as marginal total at the bottom of the matrix); N is the total number of observations included in the matrix.

In reality, \hat{k} usually ranges between 0 and 1. In the case of perfect classification, as true agreement (observed) approaches 1 and chance agreement approaches 0, \hat{k} will approach 1. In this research, the classification result \hat{k} equals 0.73. It can be thought of as an indication that an observed classification is 73 per cent better than one resulting from chance.

The \hat{k} of 0.73 is a quite promising result for the robust classification method based on waveform analysis. Moreover, we can see more interesting points in Table 2. The urban and high vegetation results are quite high in both producer's accuracy and user's accuracy (87.53% and 94.81% for urban, and 72.61% and 86.56% for high vegetation). These results could lead to the conclusion that our method is adequate for the purpose of mapping urban and high vegetation.

6. CONCLUSIONS

In this paper, we have developed a new robust method for land cover classification based on full waveform laser altimetry analysis. For this purpose the waveforms were decomposed into Gaussian components. The fitted waveform is the sum of the Gaussian components. A notion of quality of fitting is defined by comparing the residuals of the waveforms after fitting to the background noise. 95% of the waveform dataset is fitted well within 25 times σ_{N_i} of local waveform noise and within 23 times $\bar{\sigma}_N$ of overall waveform noise. Furthermore, by applying the waveform analysis for land cover classification an accuracy of classification was found of 73% compared to the CORINE classification CLC2000. The group of high vegetation and urban waveforms and the group of bareland/low vegetation and water are well separated. The classification step is done by automatic processing of the waveforms. This research suggests a new and promising way to determine land cover information. Moreover, the result derived from the waveform analysis is also useful for comparison, validation or updating of classification data obtained by other methods.

However, the method can be improved as well. There is some confusion for classifying individual classes in each group. In the group of high vegetation and urban, the classification method can be improved more to get better discrimination of between high trees and buildings. The solution of this matter is to consider the width of every Gaussian models as compared to the width of all Gaussian models. This is a potential way because the waveform reflected from buildings and other artificial objects returns a narrower signal. For high vegetation, the width is expected to be quite wider.

Furthermore, the waveform parameters are not yet good enough for discrimination between the groups of bare land/low vegetation against water. In theory, the water waveform has one mode due to the flat water surface while the bare land waveform should have more than one mode with a wider width waveform caused by slope, roughness or low vegetation. However, in practice this does not seem to hold. A further step for this discrimination is to consider other parameters such as the ratio between first mode and last mode. Moreover, water waveforms over lakes or rivers somehow show multi-modes where in theory only one mode should be present. This can be explained by the presence of artificial objects like boats or ships.

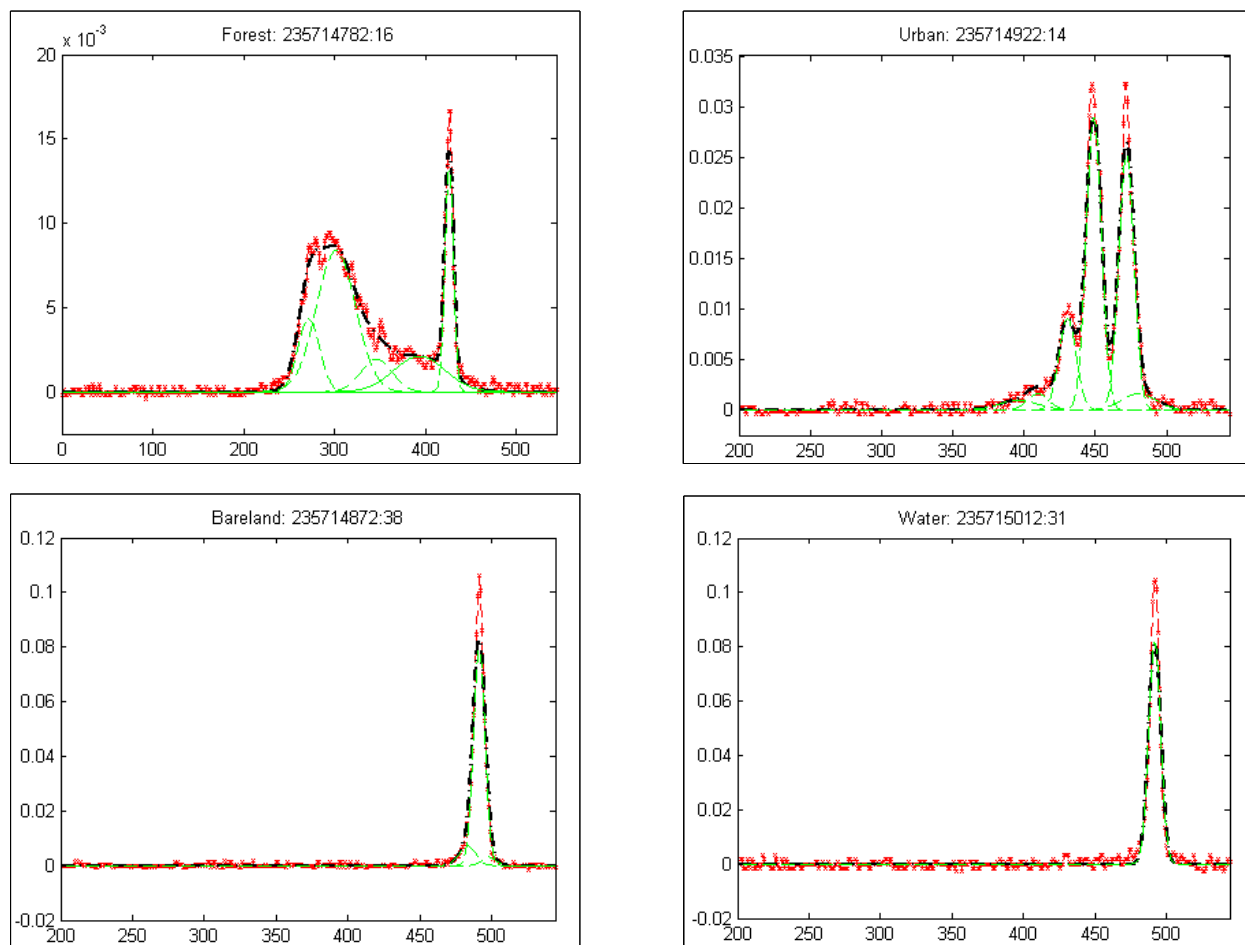


Figure 7. Top Left: High vegetation. Top Right: Urban. Bottom Left: Bare land or low vegetation. Bottom Right: Water.

Quality of fit can be incorporated into further processing of waveform data based on Gaussian decomposition, by encoding the quality in e.g. a Variance-Covariance matrix.

Finally, High Altitude Long Endurance (HALE) UAVs will maybe in future also carry lasers. With scanning mode or densely arranged profiles also laser ranging from space can be expected to provide area coverage type data in that case (Biesemans, Everaerts, and Lewyckij, 2005). The results of this paper show the feasibility of classifying on laser satellite altimetry data alone and suggest thus improved results for the combined classification of active range and passive optical imagery.

ACKNOWLEDGEMENTS

The authors would like to thank the National Snow and Ice Data Center, Hazeu from Wageningen university - the Netherlands and European Environment Agency for their guidelines and data distribution. We also would like to thank George Vosselman for his idea of checking the accuracy of the fitting method. This project is funded by the Delft Research Centre Earth.

REFERENCES

Biesemans, J., Everaerts, J., and Lewyckij, N., 2005. PEGASUS: Remote sensing from a HALE-UAV. *ASPRS annual convention*.
 CLC2000, 2006. Corine land cover 2000. *European Environment Agency*, <http://dataservice.eea.eu.int/dataservice/metadetails.asp?id=822>. last visit: 5-April-2006.

Duong, H. V., Pfeifer, N., and Lindenbergh, R., 2006. Analysis of repeated ICESat full waveform data: methodology and leaf-on / leaf-off comparison. *In Proceedings: Workshop on 3D Remote Sensing in Forestry*.

GLCN-LCTC, 2006. Historical overview of glcn-lccs. *Land cover topic centre*, <http://www.glcnlccs.org/index.php?name=Content&pa=showpage&pid=1>. last visit: 5-April-2006.

Harding, D. J. and Carabajal, C. C., 2005. ICESat waveform measurements of within-footprint topographic relief and vegetation vertical structure. *Geophysical research letters* 32, L21S10, doi:10.1029/2005GL023471.

Hazeu, G. W., 2003. CLC2000 land cover database of the Netherlands. monitoring land cover changes between 1986 and 2000. *Wageningen, Alterra, Green World Research. Alterra-rapport 775/CGI-rapport 03-006*.

Lillesand, T. M., Kiefer, R. W., and Chipman, J. W., 2004. *Remote sensing and image interpretation* (5th ed. ed.). New York: John Wiley & Sons.

NSIDC, 2006. Tools for working with icesat/glas data. *ICESat/GLAS Data at NSIDC*, <http://nsidc.org/data/icesat/tools.html>. last visit: 5-April-2006.

Ranson, K., Sun, G., Kovacs, K., and Kharuk, V., 2004. Landcover attributes from ICESat GLAS data in central Siberia. *International Geoscience and Remote Sensing Symposium, Anchorage, AK, SEP 20-24, 2004, IGARSS 2004: IEEE International Geoscience and Remote Sensing Symposium Meetings* 1-7, 753-756.